Computational Modeling of Designed Ankyrin Repeat Protein Complexes with Their Targets

Filip Radom [1], Emanuele Paci [2] and Andreas Plückthun [1]

1 - Department of Biochemistry, *University of Zurich, Zurich, Switzerland*
2 - Astbury Centre for Structural Molecular Biology, *University of Leeds, Leeds, United Kingdom*

Correspondence to Andreas Plückthun: *Department of Biochemistry, University of Zurich, 8057 Zurich, Switzerland. plueckthun@bioc.uzh.ch.*
https://doi.org/10.1016/j.jmb.2019.05.005

Abstract

Recombinant therapeutic proteins are playing an ever-increasing role in the clinic. High-affinity binding candidates can be produced in a high-throughput manner through the process of selection and evolution from large libraries, but the structures of the complexes with target protein can only be determined for a small number of them in a costly, low-throughput manner, typically by x-ray crystallography. Reliable modeling of complexes would greatly help to understand their mode of action and improve them by further engineering, for example, by designing bi-paratopic binders. Designed ankyrin repeat proteins (DARPins) are one such class of antibody mimetics that have proven useful in the clinic, in diagnostics and research. Here we have developed a standardized procedure to model DARPin–target complexes that can be used to predict the structures of unknown complexes. It requires only the sequence of a DARPin and a structure of the unbound target. The procedure includes homology modeling of the DARPin, modeling of the flexible parts of a target, rigid body docking to ensembles of the target and docking with a partially flexible backbone. For a set of diverse DARPin–target complexes tested it generated a single model of the complex that well approximates the native state of the complex. We provide a protocol that can be used in a semi-automated way and with tools that are freely available. The presented concepts should help to accelerate the development of novel biotherapeutics for scaffolds with similar properties.

Introduction

Protein–protein interactions mediate most biological processes, including structural organization of the cell, extra- and intra-cellular signaling and metabolic pathways [1–3]. The specificity of these interactions is maintained by a unique spatial arrangement of the residues that form the contacts between the molecules [4]. A single protein may interact with multiple binding partners in orthogonal ways, leading to different biological effects [5]. Therapeutic proteins that only block some of these interactions would be desirable. In other instances, receptors can be blocked by bi-paratopic therapeutic binding molecules [6] which need to interact with the receptor in precise geometric arrangements. In all of these and many other instances, a structural understanding of the interaction of the target with the binding protein would be instrumental in developing improved protein-based therapeutics.

Although *in vitro* selection methods of protein binders may promote binding to certain regions on the target protein surface, such a bias largely depends on the target, that is, if the targeted subdomains can be expressed individually and be stable during the selection, or if reagents that mask unwanted surfaces are available. Even in these favorable cases, there are usually still many possible binding geometries, and the exact epitope remains to be determined experimentally, typically by x-ray crystallography with extremely uncertain time lines. Therefore, a method to reliably predict the binding mode of protein binders that can be used routinely would greatly accelerate the development of bio-

therapeutics. Such a method would help not only to explain the binder's mode of action but also to rationally improve its design.

Predicting structures of protein complexes is still a major challenge. This is because a number of isoenergetic conformations of proteins coexist and the nature of energy functions is only approximate. A number of protein–protein docking algorithms have been developed, for example, ZDOCK [7], HADDOCK [8], PIPER [9], SwarmDock [10], GRAMM-X [11], DOCK/PIERR [12], Hex FFT [13], ATTRACT [14] and RosettaDock [15]. Their performance is periodically challenged in the Critical Assessment of Predicted Interactions (CAPRI) [16]. Whereas most of the available algorithms can, in many cases, generate several solutions including near-native ones, the near-native solutions rarely score best. Scoring remains a primary challenge, because scoring functions only roughly approximate free energy differences between different conformational states [17]. In addition, the algorithms are often trained on sets of bound complexes, where binding partners match each other perfectly (ideal but artificial lock-and-key model) [18]. Real-life docking of unbound structures that have been experimentally determined as separate proteins, or even only as homology models, where the interface is not in perfect shape complementarity to the bound partner, is much more difficult [17]. It requires different approaches, like softened energy functions to tolerate clashes or exploiting different binding models (induced-fit or conformational selection) that take into account small conformational changes upon binding [19,20].

The algorithms are typically evaluated on a diversified benchmark set that includes unbound structures of different complexes, classified as enzyme–inhibitor, antibody–antigen and others [21,22]. The best algorithms are successful in 20%–30% cases, where success is defined as finding a near-native solution within the top 10 models [17]. When only the single top-scoring model is considered, which would be the requirement to include such predictions in an actual project workflow, the success rate drops to 0–12% [17]. To improve ranking of the near-native solutions, many more re-scoring functions have been developed, but overall, they improve prediction only to a small extent [23,24].

Because of these low success rates, modeling strategies have been proposed that are individually adapted to a single complex of interest, with their success depending on modeling expertise, with an inherent risk of subjectivity, rather than being based on a reproducible procedure. Such strategies are low throughput and hence less attractive for a routine access to structural information. A general protocol that could be applied to an entire class of binders would be particularly valuable given that the number of selected binders grows too rapidly to be followed by experimental structural characterization.

The need for computational modeling of protein binders is reflected by the constant interest in antibody docking and design [25–27]. Modeling antibodies, however, is particularly challenging because their binding mode involves the interaction of six complementarity-determining loops, some of which are considerably flexible. Designed ankyrin repeat proteins (DARPins) are antibody mimetics [28] with a broad range of applications [29–30]. Analogously to antibodies, they can be selected from randomized libraries against an arbitrary target protein of choice. They are very stable, and easy to produce and to handle [28,30]. DARPins have a big potential for diagnostics and as therapeutics [31]. For instance, a DARPin can distinguish between the active and inactive active form of a kinase [32], detect tumor cells with specificity higher than the corresponding Food and Drug Administration-approved antibody [33], target adenovirus to the specific tissue [34], or induce cell-specific apoptosis [6]. At present (May 2019), several DARPins are undergoing clinical trials (ClinicalTrials.gov Identifier: NCT03418532, NCT03136653, NCT02194426, NCT03084926, NCT03539549, NCT02462486, NCT02186119, NCT02462928, NCT02181517, NCT02181504).

DARPins, with most of the advantages of antibodies as protein reagents for research and already proven in the clinic as therapeutics, constitute a favorable case for computational modeling. First, they are rigid and even their binding loops have limited conformational flexibility, which largely reduces the sampling space. Second, they are fairly small (~15–18 kDa), which significantly reduces computation times. Finally, they are structurally very similar to one another, and this simplifies homology modeling.

In this paper, we report on a general strategy that can be applied to predict the structure of DARPin–target (DT) complexes. Through extensive search for optimal parameters, we developed a procedure, involving modeling, docking and ranking of the models, that is tailored to this particular type of protein–protein complexes, without being tailored to an individual target. It consists of steps performed within the Rosetta modeling software [35] and ClusPro docking algorithm [36] and is based on newly developed scripts and new scoring and filtering approaches. We thus established a protocol that correctly predicted seven out of seven complexes, which included diverse targets of different sizes and folds, bound to DARPins derived from different selection libraries. This single protocol predicted not only near-native structures of all these complexes as single top-scoring model but importantly also the complexes that were not used in optimization. The protocol requires only the unbound structure of a target and the sequence of a DARPin and can be performed in a semi-automated way.

Table 1. Overview of the receptors used for modeling

Receptor	PDB ID of the complex (chains)	PDB ID of the unbound receptor (chain)	Fold	Cα RMSD between bound and unbound receptor (Å)		Cα RMSD between bound structure and an ensemble closest to it (Å)		Flexibility ratio[a]
				Full structure	Epitope[b]	Full structure	Epitope	
HER2_IV	4HRN (BC)	1N8Z (C, 509-579[c])	Loops (S-S)	0.67	0.60	0.47	0.71	27/80 = 34%
GFP	5MA6 (AB)	1GFL (A)	β	0.89	0.52	0.88	0.53	36/230 = 16%
IL4	4YDY (AI)	2B8U (A)	α	2.05	2.30	2.02	2.28	26/129 = 20%
KRAS	5O2S (AB)	4OBE (A)	α/β	1.31	1.38	1.27	1.42	20/169 = 12%
PLK1	2V5Q (BC)	2OWB (A)	α + β	0.63	0.52	0.62	0.52	35/294 = 12%
IL13	5KNH (DI)	1IJZ (A)	α	2.23[d]	2.78	2.13	2.65	58/113 = 52%
Cathepsin B	5MBL (AB)	6AY2 (A)	α + β	0.42	0.35	0.41	0.38	22/255 = 9%

[a] Number of flexible residues/total number of residues. All residues in 3-aa segments with RMSF >0.2 Å are considered as flexible.
[b] Defined as residues within 5 Å of any DARPin atom in bound crystal.
[c] Domain IV of the receptor.
[d] Largest flexible loop was not resolved in bound crystal structure, hence excluded from RMSD calculation.

Results

In order to optimize the modeling procedures we selected five DARPin-target (DT) complexes from the Protein Data Bank (PDB). Although there are more structures available, many of them are redundant (the same DARPin with different extensions), contain different DARPins that recognize the same or overlapping epitopes, or are complexes that contain DARPins that bind differently but still to the same target (for instance, there are 20 complex structures of a DARPin with multidrug exporter AcrB). To avoid possible biases toward DARPin sequence, epitope structure, and the target structure and fold in general, we focused on several representative complexes. We aimed to cover a broad diversity of targets as well as DARPins, although the latter are structurally similar. We looked for monomeric targets of different sizes and folds, being less than 300 amino acids in length to reduce the cost of computation (see Table 1). The DARPins contained either two or three internal repeats between the N- and C-terminal capping repeats (denoted as N2C or N3C, respectively).

We chose the following complexes: DARPin G3 bound to domain IV of human epidermal growth factor receptor 2 (HER2_IV) [37], DARPin 3g124 bound to GFP [38], DARPin 44C12V5 bound to interleukin 4 (IL4) (PDB ID: 4YDY, unpublished), DARPin K27 bound to human KRAS [39] and DARPin 3H10 bound to kinase domain of polo-like kinase-1 (PLK1) [40]. We will further refer to the DARPin as "ligand" and to its binding partner as "receptor," as is commonly done in the protein–protein docking literature.

To further test the performance of the procedure, we looked at *all* remaining DT complexes available in the PDB, with different receptors, considering those receptors that were monomeric and less than 300 amino acids in length (because such complexes were also used in optimization of the modeling steps). From among five such receptors, we chose complexes with interleukin 13 [41] (IL13; PDB ID: 5KNH) and cathepsin B (PDB ID: 5MBL, unpublished) for further tests. We also considered the remaining complexes with BCL-W [42] (PDB ID: 4K5A), aminoglycoside phosphotransferase [43] (APH; PDB ID: 2BKK) and domain I of HER2 [37] (HER2_I, PDB ID: 4HRL), but excluded them for the following reasons. BCL-W is known for its extensive flexibility, and the reported structure of BCL-W in isolation was unusual for members of the family; in fact, a DARPin binder used as a co-crystallization chaperone was discovered to stabilize BCL-W in a conformation typical for other members of the BCL-2 family [42]. Similarly, APH undergoes a significant conformational change upon binding (two helices spread to accommodate DARPin loops) [43]. Because of these a priori known conformational changes upon binding, these two complexes were considered as too challenging at the current stage and excluded from analysis (Fig. S1); the general topic of receptor flexibility and the remaining limitations will be discussed later. Modeling the complex of HER2_I would be problematic for a number of reasons. First, the binder that recognizes HER2_I constitutes an unusual exception among the known DT complexes as the flexible histidine tag, a feature introduced at the N-terminus of a DARPin for purification purposes, is in this case also involved in binding. Second, the target contains a long flexible loop, unresolved in available unbound structures, which would require an individual modeling approach—this complex was therefore considered as too challenging and excluded, too.

A simplified scheme of the modeling pipeline is depicted in Fig. 1, and its particular steps (sections in

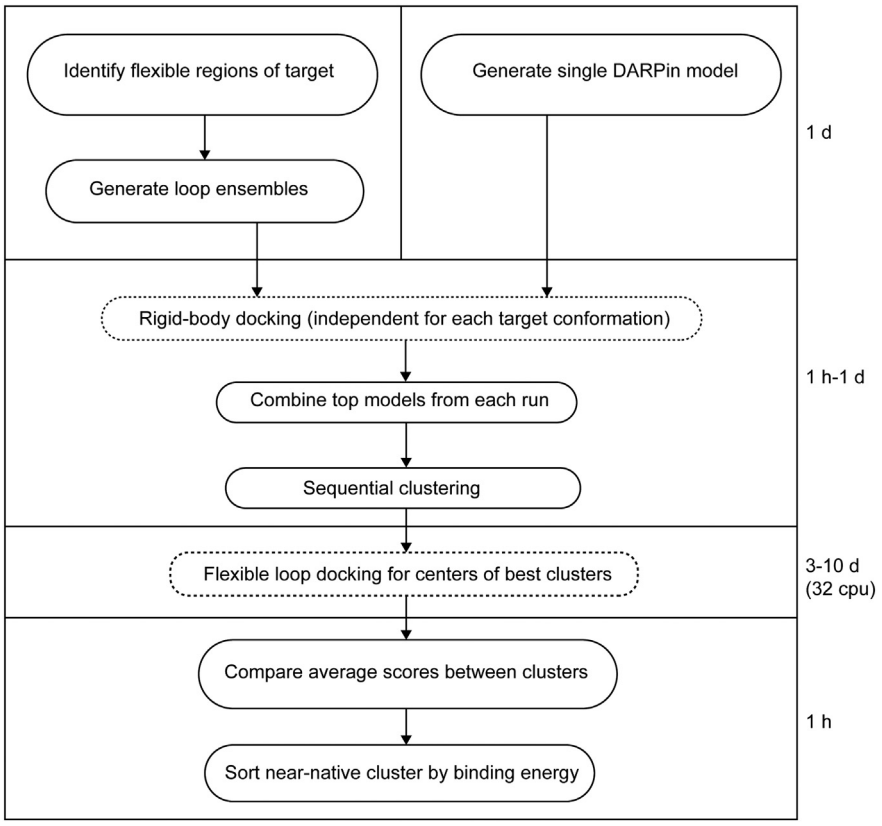

Fig. 1. Schematic protocol for modeling and docking of DARPins. The procedure can be completed within a few days. The most time-intensive step is flexible docking, which depends on the size of the receptor and the computational resources.

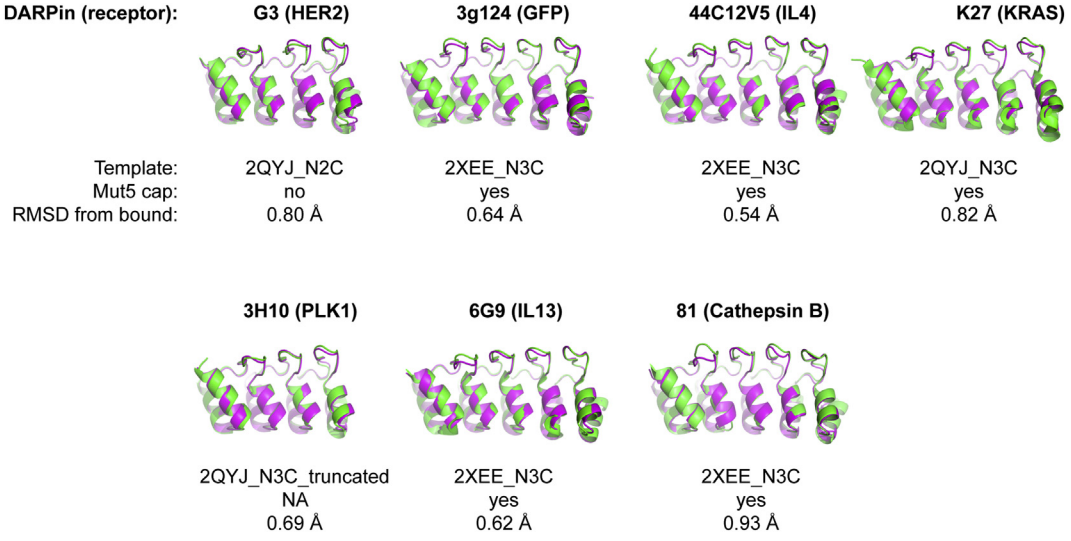

Fig. 2. Overview of homology modeling of DARPins. Diverse template structures were used for modeling, including those with two or three internal repeats (N2C or N3C) and different C-capping modules (the template derived from PDB ID: 2XEE contains the next-generation C-cap, called Mut5). Final models (magenta) were structurally aligned to crystal structures of the DARPin within the complex (green) and Cα RMSD was calculated. 3H10 (PLK1 binder) was a special case where the C-cap of the N3C template was removed (as it was experimentally shown that the cap clashes with the receptor and partially unfolds [40]).

the panel) will be described below. The detailed version of the protocol can be found in Methods and Supplementary Methods. The crystal structures of bound complexes were not used in modeling but only as evaluation of different modeling stages as well as the entire modeling success.

Homology modeling of DARPins

We developed a set of templates for DARPin modeling with Rosetta (Supplementary Files). The templates are PDB structures of consensus N3C DARPins with different caps (PDB ID:2QYJ, 2XEE), or N2C structures derived from them by removal of the second internal repeat (details in Supplementary Methods). These templates were used as input structures for fixed or flexible backbone design followed by all-atom refinement (see Methods for details). After clustering, we obtained models with <1 Å Cα RMSD from the corresponding crystal structures of the DARPin within the complex (Fig. 2). This suggests that the homology modeling of DARPins is rather straightforward because of their rigidity. As expected, the largest discrepancies occur within the loop regions.

Receptor modeling

Proteins are flexible and undergo conformational changes upon interacting with one another. Conformational changes can range from large movements, like domain reorientation or loop movements, to very small conformational adaptation of side-chain rotamers at interfaces between proteins. Because of the flexible nature of proteins, the interfaces of partners in the unbound form normally may not match each other perfectly. One of the strategies to account for protein flexibility is to consider ensembles of structures representing the variability of receptor, ligand, or both, existing in a number of different conformations. There are a number of ways to generate ensembles [44], one of them being Rosetta *backrub* [45].

To account for receptor flexibility, we developed a simple method to determine its most flexible regions that is based on Rosetta *backrub* and Pymol. We generate a number of ensembles (250) that are then structurally aligned and the protein segments of highest standard deviation of the position of each atom around the average (root mean square fluctuation, or RMSF) are calculated. With a lower RMSF cutoff of 0.2 Å, 9%–52% of receptor residues were considered as flexible (Table 1) and their backbone atoms are then allowed to be moved by Rosetta *backrub* to generate loop ensembles that are later used for docking (Fig. 3).

Interestingly, ensembles that mimic the bound state best are structurally only slightly closer to the bound state than are the unbound structures to the bound state, when entire receptors are compared. When instead only epitope similarity is considered, conformations closer to the bound state are sampled only in some cases, and the distance to the bound state does not decrease much (Table 1). How these ensembles may contribute to the docking prediction success will be discussed later.

Rigid-body docking with ClusPro

ClusPro is one of several docking servers, freely available for academic use. It is based on the PIPER algorithm that performs Fast Fourier Transform-based rigid-body docking. PIPER samples and scores billions of receptor-ligand poses [9]. The key step in ClusPro involves clustering of the best-scoring poses, assuming that the largest cluster corresponds to the broadest, and hence near-native, funnel in the binding energy landscape. ClusPro has constantly been the most successful automated server for global docking in CAPRI [36].

We use 20 loop ensembles as independent receptor inputs for ClusPro, always with the same single model of the DARPin ligand. We found that DARPin models are too similar to each other to make it worthwhile to include more models. From the different scoring functions available in ClusPro, we found the default one—called “balanced”—to be the most accurate for re-docking the bound DT complexes (unpublished). We also noticed that if the near-native solution was not present in the top 10 solutions, then it was usually not present at all (unpublished). Therefore, we consider only top 10 solutions from each run. We run ClusPro with default options, including repulsive constraints on the DARPin side, as depicted in Fig. 4, as we know that binding occurs on the concave randomized surface in all known structures.

To make the whole procedure robust and work for multiple complexes, we first spent extensive efforts to evaluate the 200 (10 each from the 20 receptor conformers) produced models (mostly using Rosetta, testing a variety of parameters and different rescoring strategies). This led us to extending the clustering approach, inspired by ClusPro itself, and we noticed that further clustering based on Cα RMSD allows to drastically narrow the pool of models to consider. We call this step sequential clustering.

Remarkably, most of the largest clusters within a 5-Å clustering radius in the optimization set were already near-native (Table 2). In one case (PLK1), the near-native cluster ranked as third. As in one case (GFP), the near-native cluster was exceptionally broad, we further clustered the pool within a smaller radius of 2 Å to identify the most populated region. In all cases, further clustering within 2 Å helped to remove many models that were more distant from the native conformation (see Average L-

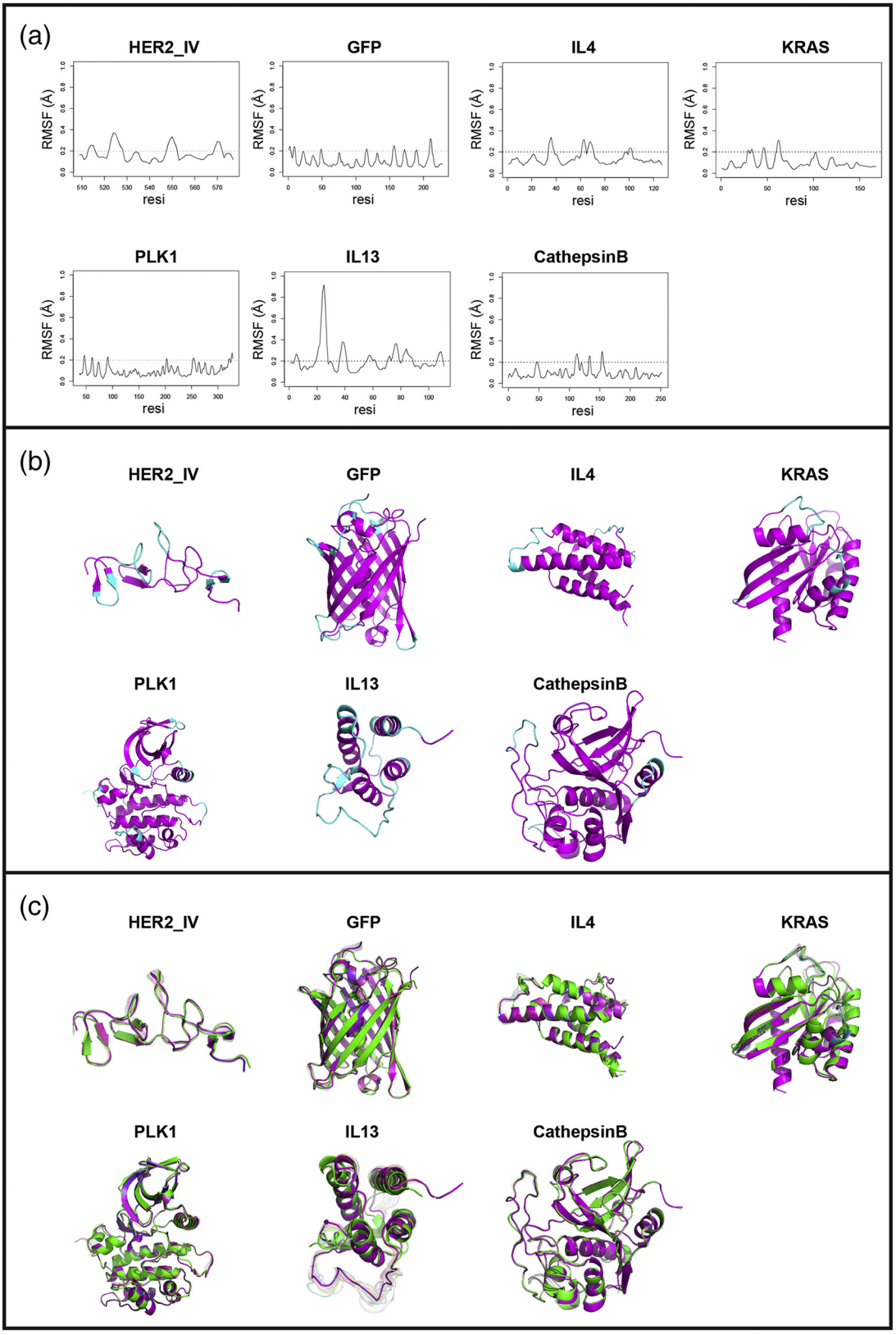
(a)
HER2_IV
GFP
IL4
KRAS
PLK1
IL13
CathepsinB
RMSF (Å)
resi
(b)
HER2_IV
GFP
IL4
KRAS
PLK1
IL13
CathepsinB
(c)
HER2_IV
GFP
IL4
KRAS
PLK1
IL13
CathepsinB

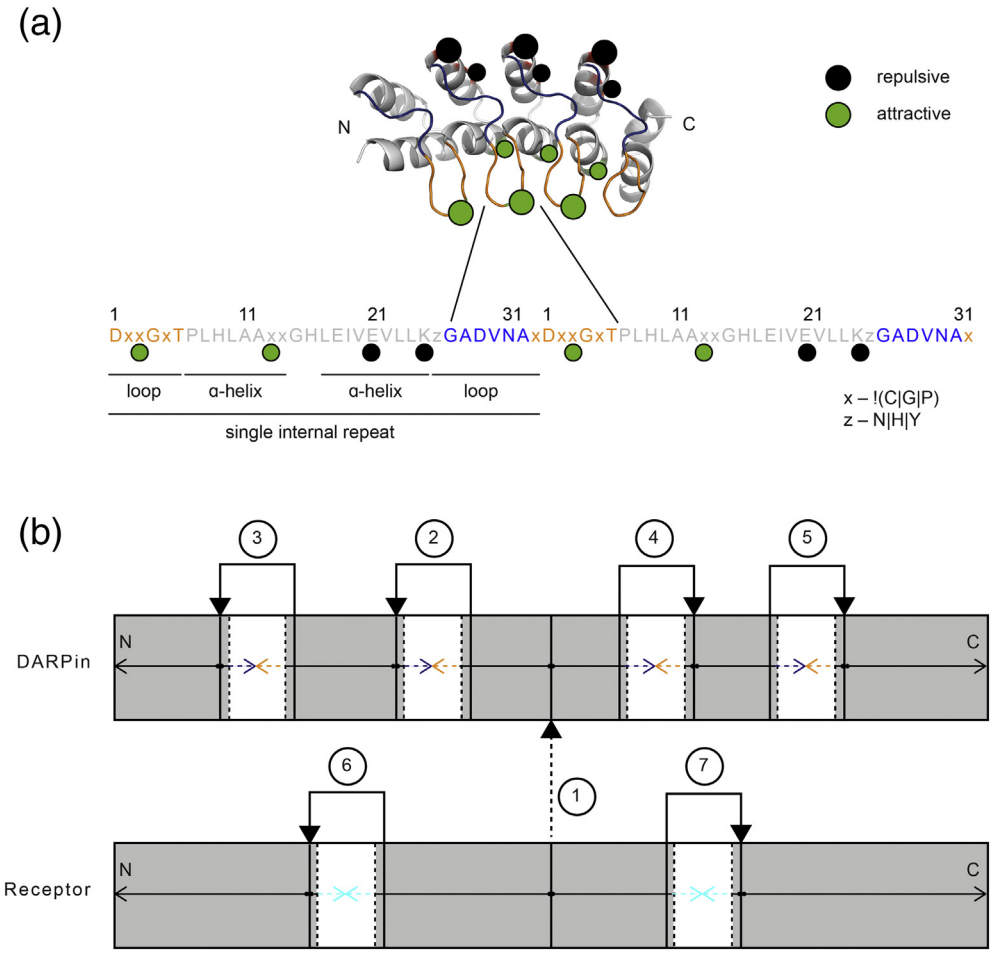

Fig. 4. Strategy for flexible docking. (a) Schematic representation of a DARPin structure. Residues constrained to be involved in interaction with the receptor or explicitly not involved are indicated as green or black spheres, respectively. Only two of the green spheres (one in α-helix and one in loop) need to be involved. (b) A scheme of relations between rigid and flexible protein fragments (fold tree) designed for flexible docking of DARPins with Rosetta. Circled are jump numbers (virtual bonds between residues). Gray regions or solid arrows indicate protein segments considered as rigid (backbone atoms). White regions with dashed lines represent flexible parts: DARPin loops (blue and orange; as in panel a) and receptor regions defined as flexible according to our Rosetta backrub-based protocol (as in Fig. 3). Note that each receptor will have a different number of flexible regions with very different spacing. Jump 1 (dashed arrow) is a connection between the centers of mass of both molecules and is also flexible (this allows motion of molecules relative to each other).

RMSD in Table 2 or Fig. S2). Whereas in most cases centers of 2-Å clusters did not change compared to centers of 5-Å clusters (suggesting a symmetric distribution of decoys around the cluster), the 2-Å center for GFP complex shifted significantly toward native from 25.5 to ~3.9 Å. Based on these observations, we considered the three largest 5-Å clusters, clustered them further within a 2 Å radius and took the centers of these sub-clusters for the next steps.

Flexible docking with Rosetta

To further account for protein flexibility, we developed a flexible docking protocol that mimics induced-fit conformational changes by including flexible loop

Fig. 3. Overview of receptor modeling. (a) RMSF of Cα atoms as a function of protein residue. Two hundred fifty full-atom ensembles generated by Rosetta *backrub* were aligned to the template structure and RMSF of 3-residue protein fragments was calculated, and is plotted as a function of the first residue of the 3-residue segment (denoted resi). (b) Regions with RMSF >0.2 Å are defined as flexible and indicated in cyan on the unbound structure of the receptor (magenta). (c) Unbound structure of the receptor (magenta) aligned to the bound structure (green). Twenty loop ensembles are indicated in other colors. For details, see Table 1.

Table 2. Overview of models at different stages

Complex	5-Å clustering				2-Å clustering			Flexible refinement
	Rank of the near-native cluster	No. of members of the near-native cluster	Average L-RMSD (Å)[a]	L-RMSD of center of largest cluster from xtal (Å)	No. of members of the largest cluster	Average L-RMSD (Å)	L-RMSD of center of largest cluster from xtal (Å)	L-RMSD from xtal of best model sorted by dG_separated (Å)
G3:HER2	1	61	10.19 ± 4.79	3.79	18	4.05 ± 1.16	3.79	3.25
3g124:GFP	1	42	15.94 ± 8.71	25.51	13	7.03 ± 2.83	3.94	4.00
44C12V5:IL4	1	34	7.46 ± 3.23	4.75	11	4.65 ± 1.55	4.75	4.33
K27:KRAS	1	62	9.25 ± 3.42	7.29	16	7.48 ± 0.76	7.29	6.56
3H10:PLK1	3	18	11.12 ± 3.01	10.85	10	11.28 ± 1.62	10.85	5.23
6G9:IL13	2	22	6.26 ± 4.09	3.24	16	4.23 ± 1.79	3.24	3.12
81:CathepsinB	3	20	8.57 ± 2.24	9.44	15	8.52 ± 1.99	9.44	8.50

[a] Ligand-RMSD (L-RMSD), of members of near-native cluster, from crystal structure. Mean ± SD.

minimization [46]. It is known that constraints, that is, any information about atoms that are involved in binding, help in docking by significantly narrowing the search space [47]. Knowing that specific DARPins invariably bind via their randomized surface, we defined a few general constraints for docking. These include repulsion at the backside of the DARPin that is not involved in interaction, and attraction at the randomized positions that usually bind the receptor (Fig. 4a). Each internal repeat of a DARPin contains randomized positions in the α-helix and in the loop, but not all of the repeats are necessarily involved in interactions. Therefore, we defined an “attractive” constraint to be satisfied if any of the chosen loop residues and any of the chosen helix residues is involved in binding. In other words, an attractive constraint would be satisfied if at least one of the repeats is involved in binding, and constitutes thus a soft condition that will normally be met.

We then built a scheme of the relations between rigid and flexible protein fragments for Rosetta—called "fold tree" [46]—where flexible segments are DARPin loops (defined as in Fig. 4a) and receptor loops, as determined above. A scheme of such a universal fold tree is shown in Fig. 4b.

We explored the local energy landscape by local flexible docking. One thousand decoys were generated for each input structure, that is, the centers of each 2-Å cluster. Since three clusters were considered for every complex to be modeled, 3000 structures in total for a single complex were modeled. We provide a template script with a sample fold tree that can be easily adapted to any DT complex, available in Supplementary Files.

Final ranking and scoring

Identifying near-native solutions in a crowd of false positives is the primary challenge in protein–protein docking [17,48]. We tried a variety of filtering and ranking approaches to identify the near-native solutions within the 3000 decoys. Our approaches were based on different Rosetta scores as well as clustering. Although many alternative strategies have worked for either one or two different complexes, they were never robust enough to succeed in more than three cases at the same time (unpublished observations).

Interestingly, Rosetta *total_score* was never a good metric to distinguish the near-native cluster, nor were scores accounting for binding energy (*dG_separated*), packing (*packstat*) or shape complementarity (*sc_value*), when considered individually. A parameter that allowed good discrimination of the near-native cluster considers all these parameters (*dG_separated*, *packstat*, *sc_value*) together, where the weight of packing is increased (by considering packing twice). We called this parameter the p2gs score (Table ST1 and Table ST2). This may

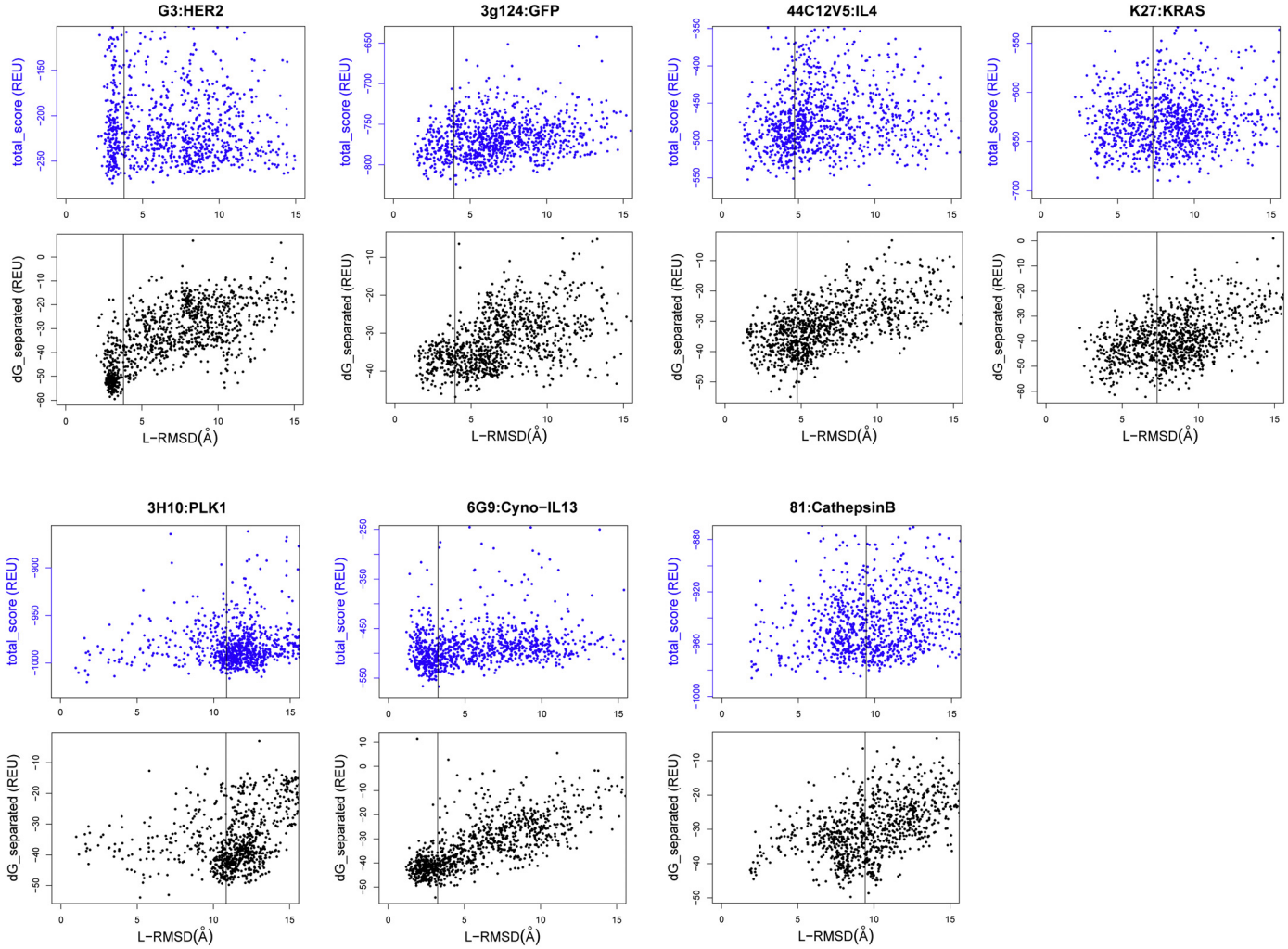

Fig. 5. Flexible docking with Rosetta. Score (*total_score*, blue plots) or binding energy (*dG_separated*, black plots) of the models from the near-native cluster as a function of L-RMSD values. In all cases, solutions closer to the crystal structure of the complex than the input model (indicated by vertical line) were generated. *Total_score* axes were scaled such that the *y*-axis midpoint is at the mean, and the axis stretches symmetrically to the observed minimum (with a further distance of 10 REU on either side) and the same distance is plotted to define the maximum (e.g., if the mean *total_score* value for the set of 1000 decoys was −400 REU and the minimal value was −500 REU, then the axis stretches from −390 to −510 REU). All *dG_separated* values within models generated for each complex are shown.

Table 3. Quality of top models sorted by binding energy or total energy

	G3:HER2	3g124:GFP	44C12V5:IL4	K27:KRAS	3H10:PLK1	6G9:IL13	81:CathepsinB
Rank dG_separated							
1	0.63/3.25/1.99[a]	0.91/4.00/1.51	0.49/4.33/2.13	0.75/6.56/2.33	0.79/5.23/1.93	0.71/3.12/1.97	0.45/8.50/2.75
2	0.67/2.94/1.98	0.91/3.07/1.31	0.68/3.06/1.79	0.77/4.53/2.07	0.75/7.11/2.66	0.66/3.49/2.21	0.43/9.68/3.16
3	0.71/3.45/2.03	0.89/4.67/1.52	0.65/3.60/1.58	0.83/4.20/1.98	0.68/11.05/2.46	0.69/2.80/1.96	0.53/8.03/2.84
4	0.67/3.08/2.00	0.89/5.43/1.62	0.46/4.55/2.21	0.62/7.50/2.50	0.74/10.61/2.49	0.66/1.88/1.90	0.53/7.84/2.71
5	0.75/3.03/1.91	0.91/2.23/1.22	0.49/4.70/2.25	0.45/8.73/2.74	0.70/12.13/3.76	0.64/4.39/2.28	0.43/10.19/3.07
6	0.75/3.64/1.98	0.89/4.85/1.63	0.47/4.90/2.33	0.65/6.00/2.66	0.81/5.41/1.87	0.71/3.73/1.97	0.68/6.41/2.23
7	0.76/3.07/1.94	0.48/5.57/3.22	0.49/4.75/2.26	0.50/9.40/3.26	0.68/11.25/2.54	0.62/4.57/2.48	0.55/7.76/2.84
8	0.65/3.20/2.08	0.87/1.86/1.29	0.62/3.70/1.68	0.83/4.30/1.96	0.60/12.41/2.72	0.71/3.17/1.86	0.42/8.37/3.29
9	0.78/2.86/1.82	0.93/3.02/1.24	0.54/5.94/2.39	0.60/7.16/2.43	0.70/10.40/2.45	0.72/2.68/1.94	0.50/8.51/2.96
10	0.67/3.42/1.93	0.48/9.82/2.90	0.65/3.18/1.64	0.50/7.86/2.36	0.57/12.32/2.63	0.67/3.55/2.16	0.63/6.89/2.26
Rank total_score							
1	0.76/3.07/1.94	0.91/4.12/1.26	0.26/9.66/4.06	0.33/9.68/2.33	0.87/1.76/0.82	0.71/3.33/1.82	0.65/6.79/2.62
2	0.57/5.72/2.85	0.89/4.74/1.43	0.60/1.73/1.37	0.48/8.46/2.07	0.70/11.07/2.69	0.67/2.28/1.88	0.82/1.99/1.13
3	0.73/2.93/1.87	0.96/3.73/1.41	0.49/4.70/2.25	0.30/7.66/1.98	0.45/13.16/3.00	0.71/2.68/1.82	0.43/9.08/3.07
4	0.71/2.90/1.92	0.93/2.31/1.22	0.65/3.60/1.58	0.70/3.72/2.50	0.77/3.56/1.66	0.66/3.13/2.05	0.65/3.26/1.52
5	0.59/4.25/2.11	0.80/5.22/2.09	0.37/7.35/2.73	0.40/8.95/2.74	0.91/1.84/0.72	0.67/2.88/2.05	0.38/8.64/2.88
6	0.63/3.12/2.03	0.89/2.19/1.37	0.34/7.11/2.54	0.32/10.95/2.66	0.43/8.41/3.13	0.67/3.03/1.90	0.40/7.80/3.18
7	0.65/3.16/2.09	0.93/3.15/1.17	0.47/3.19/1.69	0.70/6.00/3.26	0.74/10.94/2.79	0.71/2.75/1.98	0.70/6.27/2.18
8	0.57/4.17/1.69	0.87/5.66/1.70	0.56/4.29/1.74	0.40/10.37/1.96	0.68/10.85/2.40	0.66/2.71/1.83	0.77/4.86/1.62
9	0.73/2.73/2.05	0.89/4.04/1.40	0.44/5.16/2.18	0.02/17.70/2.43	0.38/11.16/2.70	0.71/3.13/2.00	0.30/10.32/3.69
10	0.61/6.67/3.15	0.89/4.12/1.52	0.68/3.06/1.79	0.62/6.41/2.36	0.53/1.21/2.76	0.72/3.10/1.80	0.77/2.30/1.28

[a] f(nat)/L-RMSD/I-RMSD. Highest value of f(nat) and lowest values of L-RMSD and I-RMSD among top 10 are underlined.

f(nat), fraction of native residue–residue contacts; calculated with 5-Å cutoff; L-RMSD, ligand RMSD; calculated on the DARPin backbone after fitting on the target; I-RMSD, interface RMSD; calculated on backbone atoms of all residues within 10 Å of the partner molecule.

CAPRI quality criteria: High quality: f(nat) $\geq$ 0.5 and (L-RMSD $\leq$1.0 OR I-RMSD $\leq$1.0); medium quality: f(nat) $\geq$ 0.3 and (1.0 $<$ L-RMSD $\leq$5 OR 1.0 $<$ I-RMSD $\leq$2.0); acceptable quality: f(nat) $\geq$ 0.1 and (5 $<$ L-RMSD $\leq$10 or 2 $<$ I-RMSD $\leq$4).

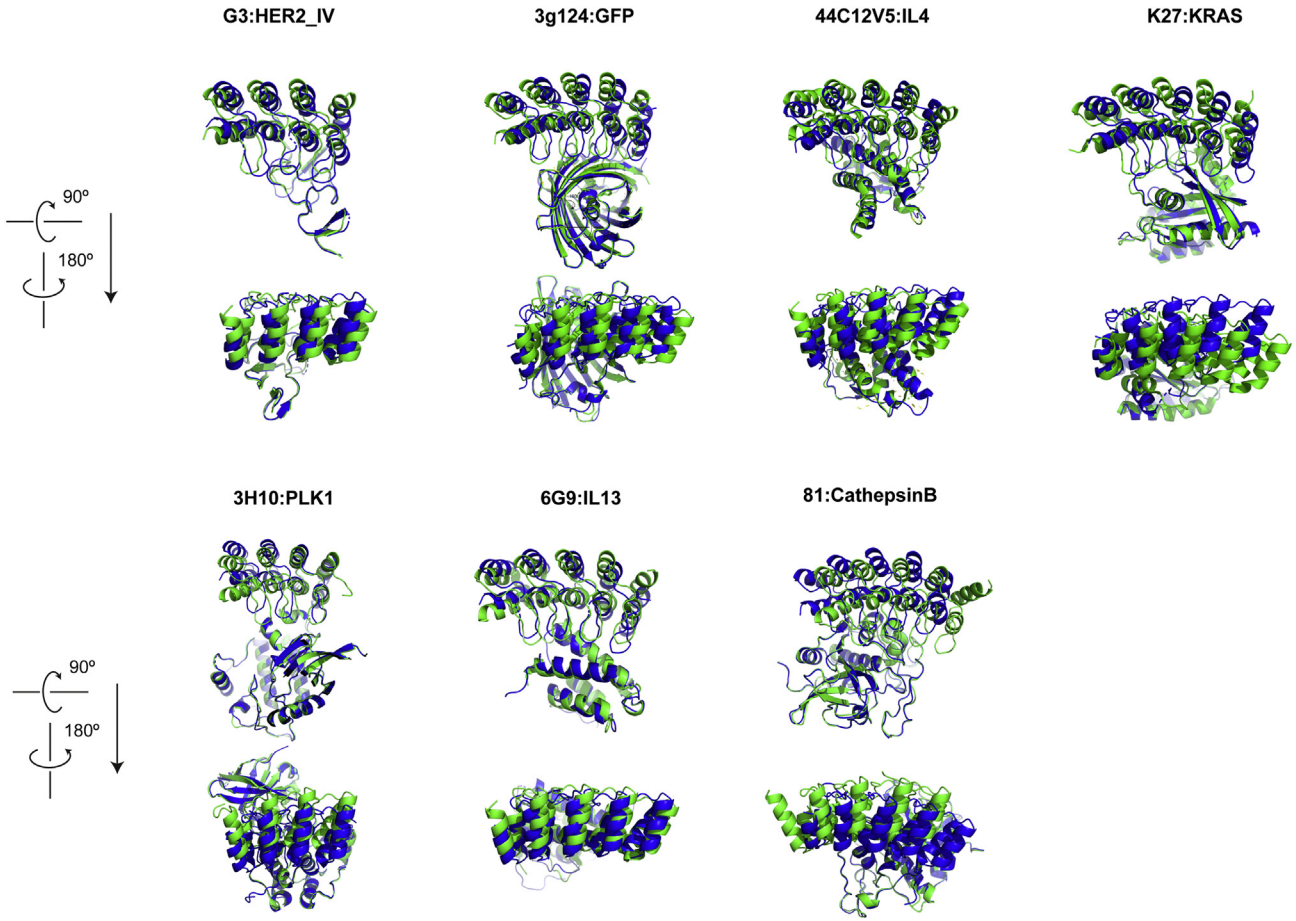

Fig. 6. Final models according to binding energy (*dG_separated*) (cf. Table 3). Models (blue) were structurally aligned to receptors in crystal structure complexes (green) to indicate the position of the DARPin (reflecting the different L-RMSD values).

be interpreted such that, according to Rosetta, the decoys around native structure have on average better binding energy, packing and shape complementarity than the decoys around a false positive structure. This also means that the other terms, many of which are knowledge-based (i.e., derived from PDB statistics), that contribute to Rosetta *total_score* are not discriminative in our cases.

In the last stage, we chose the best model from within the near-native cluster. We found the binding energy (*dG_separated*) a discriminator that was better than the total energy (*total_score*), as in most cases the correlation between *dG_separated* and RMSD was more pronounced. The energy plots for decoys generated around near-native input models are shown in Fig. 5. The top 10 decoys from each ranking (by binding or total energy) are also listed in Table 3. Interestingly, the p2gs score, which well discriminates the near-native cluster, is less accurate in ranking models *within* the near-native cluster according to their quality (Table ST3).

We computed the fraction of native contacts, ligand RMSD, and interface RMSD according to CAPRI definitions. We considered a decoy with the best binding energy, *dG_separated*, as our final model (Fig. 6, Table 3). In most cases, we obtained models better than the models after sequential clustering (see Table 2). According to CAPRI definitions, we ended up as the top scoring model for each complex with five medium quality models and two acceptable models as the single model (top line in Table 3). We consider this as a refinement success. Interestingly, in all cases, even better solutions (closer to native) were generated, but we could not find a uniform measure to identify them in all complexes.

Discussion

We developed a strategy to generate structural models of DARPin complexes with their targets, starting from the crystal structure of the unbound target and only the DARPin sequence. This is the scenario encountered when binders have been selected from a library against a target. It would offer great insight, if the epitopes and orientations of the binders on the target could be determined routinely to elucidate the molecular origin of the biological activity, or its absence.

The strategy has been optimized with structures of diverse complexes and tested on these, as well as on additional unrelated complexes. In all cases we were able to obtain a *single* model that was near-native and would be classified as “medium” or “acceptable” model according to CAPRI criteria. We found several steps of the protocol crucial for this success and will discuss them in more detail in the following paragraphs.

The first important step is sequential docking to different receptor ensembles. The ensembles are generated by exclusively varying the conformation of receptor fragments that we define as most flexible. This reduces unnecessary exploration of the structure space around rigid segments and, instead, introduces more diversity to the flexible parts at similar computational costs.

Whether ensembles may increase docking success rates has been previously discussed [19,49]. We believe that in the case of small conformational changes, where the epitope does not have to be first uncovered, or significantly move toward the bound state (insightfully discussed by Kuroda and Gray [50]), it is most important to slightly relax the epitope to probe binding. As the native complex should be in a broad energetic minimum, such small perturbations should not greatly disturb binding. On the other hand, they would hamper false positives that score well only because of particularly good local geometries, but would no longer bind even after very small movements. In other words, minor movements of the backbone at the interface should not prevent native binding but would remove some of the false positives. Indeed, among our examples, near-native models were found within models containing different receptor conformations and not just in a single conformation that was closest to the bound state, emphasizing the width of the energy funnel of the native complex. In the case of the DARPin–GFP complex, the entire native epitope was determined as rigid. Therefore, as we hypothesize, loop ensembles far from the binding region might have removed a number of false positives, since they would bind to only a single conformer. Docking 3H10 to the unbound structure of PLK1 as a control (using 20 independent ClusPro simulations, but instead of 20 target ensembles, using the same unbound structure of the target—not subjected to *backrub*) did not generate any near-native model among the 200 solutions (not shown). Sequential clustering of models containing only the ensemble of target structures (instead of the single structure) allowed narrowing the 200 models from ClusPro to the three most populated groups (clusters), one of which was in all cases near-native.

The second challenge was to distinguish the correct model out of the three highest-ranking clusters. We took the cluster centers as a starting point for high-resolution flexible docking with Rosetta. Despite individual successes with a number of diverse attempts of filtering, sorting and scoring, we strived to find a robust method that would work for all five diverse cases used for optimization and could thus form the basis for a more generic approach. We therefore came up with the idea of comparing average scores of *sets* of decoys generated from individual input structures. This approach is again based on the assumption that the near-native structure should lie in a broad funnel on the

energy landscape, and the average energy of the near-native cluster should be lower than the average energy of false positive clusters (even if *single* decoys may score better than any near-natives). In other words, false positives should score less favorably after local perturbations (because they lie in a narrow energetic minimum and thus in a narrow minimum of the scoring function).

An alternative approach of exploring the local minima of the scoring function was proposed by Kozakov *et al*. [51]. There, the stability of the cluster, corresponding to the broadness of the energy funnel, is assessed by the convergence of cluster members to a single structure after Monte Carlo-based local docking. Our approach provides an effective alternative by exploiting the same assumption about the energy landscape in a different way, which is independent of the additional uncertainty of successful convergence.

From all the different Rosetta scores, as well as the additional metrics that we introduced, the final ranking of the near-native cluster by binding energy was the most discriminative. We took the best-scoring model as the final one, but other models in the top 10 were on average similarly good (except for PLK1), and choosing a random model of these 10 would in most cases still be safe. Interestingly, Rosetta often sampled exceptionally good solutions that were less than 2 Å L-RMSD (Fig. 5), but we could not find a unified way to identify them. Nevertheless, solutions at 10 Å L-RMSD would in most cases still be a good approximation of the binder's position, sufficient to redesign the less promising candidates by rational mutagenesis, or designs of flexible or rigid linkers that often connect DARPins to each other [37], or to other functional moieties that should not interfere with binding (small-molecule drugs, dyes, PEG) [52]. On the other hand, solutions that are less than 10 Å off can often be refined by other approaches, for example, molecular dynamics [53,54].

Remarkably, even solutions as far as 10 Å L-RMSD off the native conformation captured a high fraction of native contacts, which comes as a result of side-chain and backbone flexibility. Therefore, even when the rigid body orientation is not perfect, such loops and side-chain conformations are preferred that maintain the correct residue–residue contacts. The knowledge about interacting residues may already serve for improved design by rational mutagenesis.

There are some limitations that remain. One, very vivid to the entire modeling field, is the flexibility of proteins, here limited to the target, as DARPins are rather rigid. Remarkably, in some cases, even despite quite significant conformational changes induced by binding, we could still identify near-native models. In KRAS, an entire helix shifts toward the bottom side of the DARPin. Apparently, this interaction is not critical and, most importantly, lack of this conformational change in the receptor does not prevent binding. In other cases, like APH or BCL-W, the conformational change upon binding is too massive to recapitulate it with Rosetta *backrub*, and it would be hard with other methods, too.

The change in APH seems to be very much induced by the DARPin ligand that slips in between two helices (Fig. S1). Sampling such conformations without the presence of the ligand is extremely difficult, although this state must be populated to some degree for binding to occur. The Cα RMSD between bound and unbound APH is 3.22 Å for the full structure and 4.83 Å for the epitope. We attempted to model this challenging complex with our protocol. Nevertheless, as expected, the difference between the bound and the unbound state appeared to be too large, and none of the 200 models generated by ClusPro were near-native. A key reason for this failure was that this epitope, consisting of two helices, was not recognized as flexible by the Rosetta *backrub*-based method. For this reason, we also tried to recapitulate the bound state with another recently published tool—CABS-flex 2.0 [55]. This method was trained on a database of molecular dynamics simulations and might be expected to better reflect larger conformational changes. Nevertheless, also CABS-flex 2.0 evaluated this epitope as rigid, emphasizing the challenge of sampling the rarely populated states. It is conceivable that the conformational change within the epitope becomes only energetically accessible in state already partially bound by the DARPin, which would make modeling of such complexes extremely challenging. On the other hand, bound docking in ClusPro generated a near-native solution as the first rank (Table ST4), indicating that scoring should not be a problem in this case.

BCL-W contains large flexible loops and long flexible termini, one of which covers the epitope in the unbound structure of the protein. In this case, only very harsh sampling of the loop could perhaps uncover the epitope. Interestingly, the bound structure of BCL-W makes it more similar to the structure of other BCL-2 family members [42], again suggesting that this conformation must be populated to some degree, or binders would not have been selected.

A related problem may be any structurally unresolved parts of the receptor in its unbound structure. If the missing loops are short (up to 5–6 residues), they can usually be reasonably well modeled, for example, with kinematic loop closure algorithms [56]. Otherwise, more sophisticated approaches may be necessary, for example, docking with loop rebuilding [46], which are beyond the scope of this work. It is particularly likely, though, for DARPins that the missing part of the receptor is not involved in binding, as DARPins normally bind to well-ordered regions of a protein.

Another limitation may arise at the level of scoring in ClusPro. Docking of the bound structures, although successful (defined as the presence of near-native ones among top 10) for all complexes investigated here, may not always work so well, even despite the overall rigidity of the receptor (Table ST4). For example, DARPin off7 fails in docking to maltose binding protein even when starting from the structures found in the complex, most likely because the epitope is very rich in lysines, which are statistically rare at protein–protein interfaces [57] and thus receive an associated low probability. In such a case, ClusPro would also likely fail in docking of unbound structures or homology models, which is even more demanding. Interestingly, in this particular case, the use of "antibody mode" in ClusPro, where the score function does not include the knowledge-based DARS potential [58], helps to resolve the problem (unpublished observations). We believe that a ClusPro score function could in the future be weighted for DARPin complexes, as was the case with the score function tailored to antibody complexes [59].

What fraction of DT complexes is predictable with our method largely depends on the range of conformational changes of the receptor upon binding. From the complexes that we investigated, that is, monomeric receptors of limited size—which are very often the targets used for selections—it seems that most DT complexes involving such receptors are rather rigid and are thus suitable. Nevertheless, we caution that the very fact that there is a structure of the complex in the PDB database may be a bias for the fact that the structure of the target is rather rigid.

Some estimates about the success potential of this modeling method can be derived from just examining the unbound structures. If they contain many loops that appear flexible, the chance of success decreases, simply because a DARPin may bind there and rigidify the loop upon binding. On the other hand, the binder may still recognize the rigid part of the receptor, as was the case with IL-13. Interestingly, the unbound structure for this case came from NMR, emphasizing that our modeling strategy is independent of the method used to obtain the unbound structure of the receptor.

Acknowledging the above limitations, the strategy presented here may be robust to predict a number of DT complexes, provided that the target is not too flexible. What we find especially noteworthy is that a single objective modeling protocol that can be executed without human bias can generate a single near-native model of the complex in 7 out of 7 cases that fulfilled our entry criteria, or 7 out of 10 cases, when not taking prior knowledge of conformational changes into account. This is not a standard achievement when so many modeling steps are included, and we identified a robust way to distinguish the near-native model among several candidates.

The three complexes that would not be predictable with the presented strategy are characterized by significant conformational changes upon binding, or involved a non-canonical contribution to the binding mode of a DARPin (partial contribution via the histidine tag). Nevertheless, the protocol is suitable for receptors of diverse folds and sizes, as well as DARPins of different length and with various mutations, even including deletions, and by analogy, a small insertion should not be a problem either. It does not require large computational resources, and, if these are still scarce, one could also stop after the sequential clustering, ending with three models that contain a lower-quality near-native structure. Remarkably, we did not use any biochemical data at all to navigate docking, although it was available. Often, information from mutagenesis studies, competition studies, or HDX/MS could further narrow the number of model candidates and improve the prediction quality.

Finally, although the strategy was optimized with and for DARPins, we neither modified the energy functions nor included any known DARPin-specific statistical potentials. Therefore, it is likely that the approach, including ensemble docking with sequential clustering, as well as comparing average p2gs score of clusters in Rosetta could be extended to other protein–protein complexes, especially those including other rigid protein scaffolds, for example, like leucine-rich repeat proteins or affibodies.

Methods

Software and hardware

Rosetta 3 [35] (version 59,812), the ClusPro docking server [36] and Pymol 2.1.0 (Schrödinger) were used for modeling, docking and analysis. R software [60] was used to analyze data.

Modeling

The full detailed protocol which was used for every complex in this study is described in Supplementary Information. All templates and scripts are available at https://github.com/ThePlueckthunLab/DARPin_Docking.

Briefly, PDB structures 2QYJ, 2XEE and their derivatives (see Supplementary Methods for details) were used as templates for homology modeling of DARPins with Rosetta. Desired mutations were introduced with fixed backbone design [61] or, when loop insertion was necessary, with the flexible backbone design protocol [62]. Models were refined with *Rosetta.relax* [63] in 40 independent trajectories, and the models were clustered within 0.2-Å

radius in *Rosetta.cluster*. The best scoring model of the largest cluster was considered further.

The unbound structure of the target (receptor) was subjected to *Rosetta.backrub* [64]. Two hundred fifty generated ensembles were structurally aligned, and the Cα RMSF of the 3-residue protein segments were calculated. Residues in segments with RMSF >0.2 Å were considered as flexible. Twenty loop ensembles of the target were generated with *Rosetta.backrub* performed exclusively on flexible parts.

Rigid body docking was performed in ClusPro, with a single DARPin model and the 20 target ensembles individually. Repulsive constraints on the DARPin side were included. The top 10 solutions of each simulation were combined (200 models) and clustered sequentially with *Rosetta.cluster*: three largest clusters within 5 Å radius were further clustered within 2 Å radius and the centers of these clusters were considered further in flexible docking.

Flexible docking was performed in Rosetta with a custom Rosetta script [65], available in Supplementary Files. It was based on Wang *et al.* [46], the synthesis of valuable suggestions from the RosettaCommons community (https://www.rosettacommons.org/forum) and further optimization. Protein segments considered as flexible were receptor loops, as determined above, and DARPin loops (details in Supplementary Information). Site constraints in the functional form of $(1/(1 + \exp(-m^*(x-x0))) - 0.5)$ were used throughout the simulation, where $x0$ is the center of the sigmoid function and m is the slope. The constraints were centered at 8 Å. Repulsive constraints had a slope set to −2.0. Attractive constraints had a slope set to +2.0 and were wrapped up into *KofNConstraints*, where at least one condition had to be satisfied for the *KofNConstraint* to be satisfied. The constraints were applied at a weight = 5 to both low- and high-resolution docking stages. The initial pose of the ligand was perturbed along the vector connecting the centers of mass of the two proteins and around its axis (Gaussian distribution around 3 Å and 8°). Low-resolution, rigid body docking was performed as in Gray *et al.* [15]. This was followed by 50 cycles of high-resolution Monte-Carlo minimization. Each cycle consisted of a random perturbation (Gaussian distribution around 0.1 Å and 3°), repacking, minimization of side chains at interface, repacking and minimization of backbone and side chains of segments defined as flexible. For all minimization steps within the cycle, the *Ref2015* score function was used [66]. A single Monte-Carlo minimization cycle was evaluated using the Metropolis criterion on the *docking* score function [48]. An example of constraint file, fold tree and the full script can be found in the Supplementary Files. Flexible docking in Rosetta was performed for each of the three model candidates (after sequential clustering) as input, generating 3 × 1000 new models. All decoys were analyzed with *Rosetta.InterfaceAnalyzer*, and the average p2gs score for sets of models derived from different inputs were compared.

Acknowledgments

Computations were performed with infrastructure provided by S3IT, the Service and Support for Science IT team at the University of Zurich (www.s3it.uzh.ch). We thank Hamed Khakzad and Dr. Lars Malmström for the help with setting up Rosetta on a computer cluster, Dr. Annemarie Honegger for valuable discussions, and K. Patricia Hartmann and Dr. Markus Schmid for critical reading of the manuscript. This work was supported by the Schweizerischer Nationalfonds (Grant 310030B_166676; to A.P.)

Appendix A. Supplementary data

Supplementary data to this article can be found online at https://doi.org/10.1016/j.jmb.2019.05.005.

Received 26 February 2019;
Received in revised form 3 May 2019;
Available online 11 May 2019

Keywords:
DARPin;
protein–protein docking;
homology modeling;
Rosetta;
ClusPro

Abbreviations used:
CAPRI, Critical Assessment of Predicted Interactions; DARPins, designed ankyrin repeat proteins; DT, DARPin–target; PDB, Protein Data Bank; RMSF, root mean square fluctuation; RMSD, root mean square deviation.

References

[1] T.S. Lewis, P.S. Shapiro, N.G. Ahn, Signal transduction through MAP kinase cascades, Adv. Cancer Res. 74 (1998) 49–139.
[2] A.R. Saltiel, C.R. Kahn, Insulin signalling and the regulation of glucose and lipid metabolism, Nature 414 (2001) 799–806.
[3] H. Vindin, P. Gunning, Cytoskeletal tropomyosins: choreographers of actin filament functional diversity, J. Muscle Res. Cell Motil. 34 (2013) 261–274.
[4] S. Jones, J.M. Thornton, Principles of protein–protein interactions, Proc. Natl. Acad. Sci. U. S. A. 93 (1996) 13–20.
[5] A. Patil, K. Kinoshita, H. Nakamura, Hub promiscuity in protein–protein interaction networks, Int. J. Mol. Sci. 11 (2010) 1930–1943.

[6] R. Tamaskovic, M. Schwill, G. Nagy-Davidescu, C. Jost, D.C. Schaefer, W.P. Verdurmen, et al., Intermolecular biparatopic trapping of ErbB2 prevents compensatory activation of PI3K/AKT via RAS-p110 crosstalk, Nat. Commun. 7 (2016), 11672.
[7] R. Chen, L. Li, Z. Weng, ZDOCK: an initial-stage protein-docking algorithm, Proteins 52 (2003) 80–87.
[8] C. Dominguez, R. Boelens, A.M. Bonvin, HADDOCK: a protein–protein docking approach based on biochemical or biophysical information, J. Am. Chem. Soc. 125 (2003) 1731–1737.
[9] D. Kozakov, R. Brenke, S.R. Comeau, S. Vajda, PIPER: an FFT-based protein docking program with pairwise potentials, Proteins 65 (2006) 392–406.
[10] I.H. Moal, P.A. Bates, Swarmdock and the use of normal modes in protein–protein docking, Int. J. Mol. Sci. 11 (2010) 3623–3648.
[11] A. Tovchigrechko, I.A. Vakser, GRAMM-X public web server for protein–protein docking, Nucleic Acids Res. 34 (2006) W310–W314.
[12] S. Viswanath, D.V. Ravikant, R. Elber, DOCK/PIERR: web server for structure prediction of protein–protein complexes, Methods Mol. Biol. 1137 (2014) 199–207.
[13] D.W. Ritchie, V. Venkatraman, Ultra-Fast FFT protein docking on graphics processors, Bioinformatics 26 (2010) 2398–2405.
[14] M. Zacharias, ATTRACT: protein–protein docking in CAPRI using a reduced protein model, Proteins 60 (2005) 252–256.
[15] J.J. Gray, S. Moughon, C. Wang, O. Schueler-Furman, B. Kuhlman, C.A. Rohl, et al., Protein–protein docking with simultaneous optimization of rigid-body displacement and side-chain conformations, J. Mol. Biol. 331 (2003) 281–299.
[16] M.F. Lensink, S. Velankar, A. Kryshtafovych, S.Y. Huang, D. Schneidman-Duhovny, A. Sali, et al., Prediction of homoprotein and heteroprotein complexes by protein docking and template-based modeling: a CASP–CAPRI experiment, Proteins 84 (Suppl. 1) (2016) 323–348.
[17] S.Y. Huang, Exploring the potential of global protein–protein docking: an overview and critical assessment of current programs for automatic ab initio docking, Drug Discov. Today 20 (2015) 969–977.
[18] S. Vajda, D.R. Hall, D. Kozakov, Sampling and scoring: a marriage made in heaven, Proteins 81 (2013) 1874–1884.
[19] S. Chaudhury, J.J. Gray, Conformer selection and induced fit in flexible backbone protein–protein docking using computational and NMR ensembles, J. Mol. Biol. 381 (2008) 1068–1087.
[20] F. Jiang, S.H. Kim, Soft docking: matching of molecular surface cubes, J. Mol. Biol. 219 (1991) 79–102.
[21] H. Hwang, T. Vreven, J. Janin, Z. Weng, Protein–protein docking benchmark version 4.0, Proteins 78 (2010) 3111–3114.
[22] T. Vreven, I.H. Moal, A. Vangone, B.G. Pierce, P.L. Kastritis, M. Torchala, et al., Updates to the integrated protein–protein interaction benchmarks: docking benchmark version 5 and affinity benchmark version 2, J. Mol. Biol. 427 (2015) 3031–3041.
[23] D. Barradas-Bautista, I.H. Moal, J. Fernández-Recio, A systematic analysis of scoring functions in rigid-body protein docking: the delicate balance between the predictive rate improvement and the risk of overtraining, Proteins 85 (2017) 1287–1297.
[24] I.H. Moal, M. Torchala, P.A. Bates, J. Fernández-Recio, The scoring of poses in protein–protein docking: current capabilities and future directions, BMC Bioinformatics 14 (2013) 286.
[25] D. Baran, M.G. Pszolla, G.D. Lapidoth, C. Norn, O. Dym, T. Unger, et al., Principles for computational design of binding antibodies, Proc. Natl. Acad. Sci. U. S. A. 114 (2017) 10900–10905.
[26] S. Fischman, Y. Ofran, Computational design of antibodies, Curr. Opin. Struct. Biol. 51 (2018) 156–162.
[27] B.D. Weitzner, J.R. Jeliazkov, S. Lyskov, N. Marze, D. Kuroda, R. Frick, et al., Modeling and docking of antibody structures with Rosetta, Nat. Protoc. 12 (2017) 401–416.
[28] H.K. Binz, M.T. Stumpp, P. Forrer, P. Amstutz, A. Plückthun, Designing repeat proteins: well-expressed, soluble and stable proteins from combinatorial libraries of consensus ankyrin repeat proteins, J. Mol. Biol. 332 (2003) 489–503.
[29] P. Forrer, M.T. Stumpp, H.K. Binz, A. Plückthun, A novel strategy to design binding molecules harnessing the modular nature of repeat proteins, FEBS Lett. 539 (2003) 2–6.
[30] H.K. Binz, P. Amstutz, A. Kohl, M.T. Stumpp, C. Briand, P. Forrer, et al., High-affinity binders selected from designed ankyrin repeat protein libraries, Nat. Biotechnol. 22 (2004) 575–582.
[31] A. Plückthun, Designed ankyrin repeat proteins (DARPins): binding proteins for research, diagnostics, and therapy, Annu. Rev. Pharmacol. Toxicol. 55 (2015) 489–511.
[32] P. Parizek, L. Kummer, P. Rube, A. Prinz, F.W. Herberg, A. Plückthun, Designed ankyrin repeat proteins (DARPins) as novel isoform-specific intracellular inhibitors of c-Jun N-terminal kinases, ACS Chem. Biol. 7 (2012) 1356–1366.
[33] J.P. Theurillat, B. Dreier, G. Nagy-Davidescu, B. Seifert, S. Behnke, U. Zurrer-Hardi, et al., Designed ankyrin repeat proteins: a novel tool for testing epidermal growth factor receptor 2 expression in breast cancer, Mod. Pathol. 23 (2010) 1289–1297.
[34] M. Schmid, P. Ernst, A. Honegger, M. Suomalainen, M. Zimmermann, L. Braun, et al., Adenoviral vector with shield and adapter increases tumor specificity and escapes liver and immune control, Nat. Commun. 9 (2018) 450.
[35] A. Leaver-Fay, M. Tyka, S.M. Lewis, O.F. Lange, J. Thompson, R. Jacak, et al., ROSETTA3: an object-oriented software suite for the simulation and design of macromolecules, Methods Enzymol. 487 (2011) 545–574.
[36] D. Kozakov, D.R. Hall, B. Xia, K.A. Porter, D. Padhorny, C. Yueh, et al., The ClusPro web server for protein–protein docking, Nat. Protoc. 12 (2017) 255–278.
[37] C. Jost, J. Schilling, R. Tamaskovic, M. Schwill, A. Honegger, A. Plückthun, Structural basis for eliciting a cytotoxic effect in HER2-overexpressing cancer cells via binding to the extracellular domain of HER2, Structure 21 (2013) 1979–1991.
[38] S. Hansen, J.C. Stüber, P. Ernst, A. Koch, D. Bojar, A. Batyuk, et al., Design and applications of a clamp for green fluorescent protein with picomolar affinity, Sci. Rep. 7 (2017), 16292.
[39] S. Guillard, P. Kolasinska-Zwierz, J. Debreczeni, J. Breed, J. Zhang, N. Bery, et al., Structural and functional characterization of a DARPin which inhibits Ras nucleotide exchange, Nat. Commun. 8 (2017), 16111.
[40] T.M. Bandeiras, R.C. Hillig, P.M. Matias, U. Eberspaecher, J. Fanghanel, M. Thomaz, et al., Structure of wild-type Plk-1 kinase domain in complex with a selective DARPin, Acta Crystallogr. D Biol. Crystallogr. 64 (2008) 339–353.
[41] A. Teplyakov, T.J. Malia, G. Obmolova, S.A. Jacobs, K.T. O'Neil, G.L. Gilliland, Conformational flexibility of an anti-IL-13 DARPin, Protein Eng. Des. Sel. 30 (2017) 31–37.

[42] J. Schilling, J. Schöppe, E. Sauer, A. Plückthun, Co-crystallization with conformation-specific designed ankyrin repeat proteins explains the conformational flexibility of BCL-W, J. Mol. Biol. 426 (2014) 2346–2362.
[43] A. Kohl, P. Amstutz, P. Parizek, H.K. Binz, C. Briand, G. Capitani, et al., Allosteric inhibition of aminoglycoside phosphotransferase by a designed ankyrin repeat protein, Structure 13 (2005) 1131–1141.
[44] J.A. Davey, R.A. Chica, Improving the accuracy of protein stability predictions with multistate design using a variety of backbone ensembles, Proteins 82 (2014) 771–784.
[45] I.W. Davis, W.B. Arendall 3rd, D.C. Richardson, J.S. Richardson, The backrub motion: how protein backbone shrugs when a sidechain dances, Structure 14 (2006) 265–274.
[46] C. Wang, P. Bradley, D. Baker, Protein–protein docking with backbone flexibility, J. Mol. Biol. 373 (2007) 503–519.
[47] E.S. Shih, M.J. Hwang, On the use of distance constraints in protein–protein docking computations, Proteins 80 (2012) 194–205.
[48] S. Chaudhury, M. Berrondo, B.D. Weitzner, P. Muthu, H. Bergman, J.J. Gray, Benchmarking and analysis of protein docking performance in Rosetta V3.2, PLoS One 6 (2011), e22477.
[49] R. Grünberg, J. Leckner, M. Nilges, Complementarity of structure ensembles in protein–protein binding, Structure 12 (2004) 2125–2136.
[50] D. Kuroda, J.J. Gray, Pushing the backbone in protein–protein docking, Structure 24 (2016) 1821–1829.
[51] D. Kozakov, O. Schueler-Furman, S. Vajda, Discrimination of near-native structures in protein–protein docking by testing the stability of local minima, Proteins 72 (2008) 993–1004.
[52] R. Tamaskovic, M. Simon, N. Stefan, M. Schwill, A. Plückthun, Designed ankyrin repeat proteins (DARPins) from research to therapy, Methods Enzymol. 503 (2012) 101–134.
[53] F. Michael, Computational protein structure refinement: almost there, yet still so far to go, Wiley Interdiscip. Rev. Comput. Mol. Sci. 7 (2017), e1307.
[54] F. Radom, A. Plückthun, E. Paci, Assessment of ab initio models of protein complexes by molecular dynamics, PLoS Comput. Biol. 14 (2018), e1006182.
[55] A. Kuriata, A.M. Gierut, T. Oleniecki, M.P. Ciemny, A. Kolinski, M. Kurcinski, et al., Cabs-Flex 2.0: a web server for fast simulations of flexibility of protein structures, Nucleic Acids Res. 46 (2018) W338–W343.
[56] A. Stein, T. Kortemme, Improvements to robotics-inspired conformational sampling in Rosetta, PLoS One 8 (2013), e63090.
[57] C. Yan, F. Wu, R.L. Jernigan, D. Dobbs, V. Honavar, Characterization of protein–protein interfaces, Protein J. 27 (2008) 59–70.
[58] G.Y. Chuang, D. Kozakov, R. Brenke, S.R. Comeau, S. Vajda, DARS (decoys as the reference state) potentials for protein–protein docking, Biophys. J. 95 (2008) 4217–4227.
[59] R. Brenke, D.R. Hall, G.Y. Chuang, S.R. Comeau, T. Bohnuud, D. Beglov, et al., Application of asymmetric statistical potentials to antibody–protein docking, Bioinformatics 28 (2012) 2608–2614.
[60] R Development Core Team, R: A Language and Environment for Statistical Computing, R Foundation for Statistical Computing, Vienna, Austria, 2011 , ISBN: 3-900051-07-0. Available online at http://www.R-project.org/.
[61] B. Kuhlman, G. Dantas, G.C. Ireton, G. Varani, B.L. Stoddard, D. Baker, Design of a novel globular protein fold with atomic-level accuracy, Science 302 (2003) 1364–1368.
[62] P.S. Huang, Y.E. Ban, F. Richter, I. Andre, R. Vernon, W.R. Schief, et al., RosettaRemodel: a generalized framework for flexible backbone protein design, PLoS One 6 (2011), e24109.
[63] L.G. Nivón, R. Moretti, D. Baker, A pareto-optimal refinement method for protein design scaffolds, PLoS One 8 (2013), e59004.
[64] C.A. Smith, T. Kortemme, Backrub-like backbone simulation recapitulates natural protein conformational variability and improves mutant side-chain prediction, J. Mol. Biol. 380 (2008) 742–756.
[65] S.J. Fleishman, A. Leaver-Fay, J.E. Corn, E.M. Strauch, S.D. Khare, N. Koga, et al., RosettaScripts: a scripting language interface to the Rosetta macromolecular modeling suite, PLoS One 6 (2011), e20161.
[66] R.F. Alford, A. Leaver-Fay, J.R. Jeliazkov, M.J. O'Meara, F. P. DiMaio, H. Park, et al., The Rosetta all-atom energy function for macromolecular modeling and design, J. Chem. Theory Comput. 13 (2017) 3031–3048.